[CANCER RESEARCH 61, 5010–5015, July 1, 2001]

Qualitative and Quantitative Relationship between Dysplastic Aberrant Crypt Foci and Tumorigenesis in the *Min*/+ Mouse Colon

Jan Erik Paulsen, Inger-Lise Steffensen, Else Marit Løberg, Trine Husøy, Ellen Namork, and Jan Alexander[1]

Department of Environmental Medicine, National Institute of Public Health, 0403 Oslo [J. E. P., I-L. S., T. H., E. N., J. A.], and Department of Pathology, Ullevål University Hospital, N-0407 Oslo [E. M. L.], Norway

ABSTRACT

The multiple intestinal neoplasia (*Min*)/+ mouse, which harbors only one functional allele of the *Apc* gene, is susceptible to environmental factors that disrupt this gene and subsequently trigger Apc-driven tumorigenesis in the colon. Aberrant crypt foci (ACF) are assumed to be preneoplastic lesions in colon carcinogenesis. Recently, we reported the absence of "classical" ACF in the colon of untreated *Min*/+ mice. Instead we identified flat dysplastic lesions, which we denoted ACF_{Min} (J. E. Paulsen *et al.*, Scand. J. Gastroenterol., *35:* 534–539, 2000). In contrast to the classical type, ACF_{Min} are not elevated above the surrounding mucosa, and their detection is totally dependent on methylene blue staining and transillumination. In the present study, we treated *Min*/+ mice with 5 mg/kg body weight azoxymethane (AOM) at weeks 1 and 2 and demonstrated induction of both types of lesions. However, only ACF_{Min} appeared to be associated with the development of adenomas. Monocryptal ACF_{Min}, large ACF_{Min}, and adenomas showed a uniform histopathological picture of dysplasia and cytoplasmic overexpression of β-catenin, indicating a qualitative relationship between these lesions. Also a quantitative relationship was suggested because the dramatic decrease in ACF_{Min} number from week 7 to 11 was paralleled by a reciprocal increase in tumor number, indicating fast-crypt multiplication of ACF_{Min}. In AOM-treated +/+ (wild-type) littermates, a low number of ACF_{Min} and tumors with the same characteristics as in *Min*/+ mice was seen. In contrast to ACF_{Min}, histopathological and immunohistochemical examination of classical ACF showed normal or hyperplastic crypts with normal levels of β-catenin expression. In AOM-treated *Min*/+ mice, the number of classical ACF was virtually constant from week 7 to 11, and only a modest increase of crypt multiplicity was observed. The number of AOM-induced classical ACF at week 11 was not different in *Min*/+ mice and +/+ mice. In conclusion, we identified two distinct populations of altered crypts in the colon of *Min*/+ mice after AOM treatment. The ACF_{Min}, which resemble the dysplastic ACF described previously, clearly showed a continuous development from the monocryptal stage to adenoma, and they were characterized by fast-growing crypts with altered control of β-catenin. In contrast, the classical ACF, which resemble the hyperplastic ACF described previously, were characterized by slow-growing crypts with normal β-catenin expression, and they were probably not related to tumorigenesis.

INTRODUCTION

FAP,[2] an inherited form of human colon cancer, is caused by germ-line mutations in the tumor suppressor gene, *APC*. FAP is characterized by the development of hundreds to thousands of adenomas in the large intestine. If not removed, some of these lesions inevitably progress to carcinomas (1). In addition, somatic mutations in the *APC* gene are found in 85% of sporadic colorectal cancers (1, 2). Various germ-line mutations in the murine *Apc*, which is homologous to the human *APC*, cause multiple intestinal neoplasia in mice (3). *Min*/+ mice are heterozygous for a nonsense mutation in the *Apc* gene at codon 850 (4). In both FAP and *Min*/+ mice the intestinal tumorigenesis seems to be dependent on somatic genetic events that lead to the inactivation of both alleles (5–7). Loss of APC function precludes the post-translational down-regulation of β-catenin, which consequently accumulates in cytoplasm and translocates into the nucleus where it complexes with the transcription factor Tcf-4 and activates specific genes such as c-*MYC* and *cyclinD1*. Increased levels and biological activity of free β-catenin may also result from a mutated *β-catenin* gene (3).

ACF, putative preneoplastic lesions in the colon of carcinogen-treated rodents, have been used as a short-term bioassay to evaluate the role of nutritional components and chemopreventive agents at an early stage of colon carcinogenesis (8). They are scored by light microscopic examination of the mucosal surface and have also been identified in patients with sporadic colorectal cancer and patients with FAP (9). Although ACF share many morphological, genetic, and biochemical features with colonic tumors (7, 10), there is not a simple association between ACF formation and tumorigenesis. In carcinogen-treated rodents, a negative correlation between ACF formation and tumor formation (11) and a discrepancy between distribution of ACF and distribution of tumors (12) is even reported. In carcinogen-treated rodents and patients with sporadic colorectal cancer, the number of tumors is minuscule compared with the large number of ACF, indicating that only a very small fraction of ACF progresses to the stage of a tumor (9, 11). This is consistent with the observation that a large fraction of ACF is hyperplastic whereas only a small fraction of ACF shows dysplasia, a hallmark of malignant potential (9, 13). In contrast, most ACF in FAP patients are dysplastic, and their histopathology resembled that of the numerous adenomas developing (9). It has been proposed that only the dysplastic ACF progress to adenomas and adenocarcinomas (7) and that these lesions are closely related to *APC* mutations. In AOM-treated rats, small dysplastic lesions undetectable as ACF by surface examination and with *β-catenin* gene mutations have been described in histopathological sections (14). Such mutations were also observed in rat and mouse colonic tumors (15, 16). Increased expression of β-catenin has been reported in colonic tumors of AOM-treated mice and in spontaneous intestinal tumors of *Min*/+ mice (17).

Contrary to the hypothesis that ACF are preneoplastic lesions, we did not observe spontaneous formation of such classical ACF in the colon of *Min*/+ mice (18), although we demonstrated preliminarily that classical ACF may be formed in AOM-treated *Min*/+ mice (19). However, in untreated *Min*/+ mice we discovered small lesions of a different type, which we denoted ACF_{Min}. In contrast to classical ACF, these lesions were not elevated above the surrounding mucosa, and their detection was totally dependent on methylene blue staining and transillumination. ACF_{Min} exhibited dysplastic crypts similar to those found in adenomas. Also, the C57Bl/6J background of *Min*/+ mice is susceptible to AOM-induced ACF formation (20).

The aim of the present work was to monitor the development of classical ACF and ACF_{Min} in the colon of AOM-treated *Min*/+ mice to evaluate their role as potential precursors of adenomas. To ensure

Received 11/28/00; accepted 4/30/01.

The costs of publication of this article were defrayed in part by the payment of page charges. This article must therefore be hereby marked *advertisement* in accordance with 18 U.S.C. Section 1734 solely to indicate this fact.

[1] To whom requests for reprints should be addressed, at Department of Environmental Medicine, National Institute of Public Health, P.O. Box 4404 Nydalen, 0403 Oslo, Norway. Phone: 47-22-04-22-00; Fax: 47-22-04-22-43; E-mail: jan.alexander@folkehelsa.no.

[2] The abbreviations used are: FAP, familial adenomatous polyposis; AOM, azoxymethane; ACF, aberrant crypt foci; Min, multiple intestinal neoplasia; Apc, adenomatous polyposis coli; LM, light microscope; SEM, scanning electron microscope.

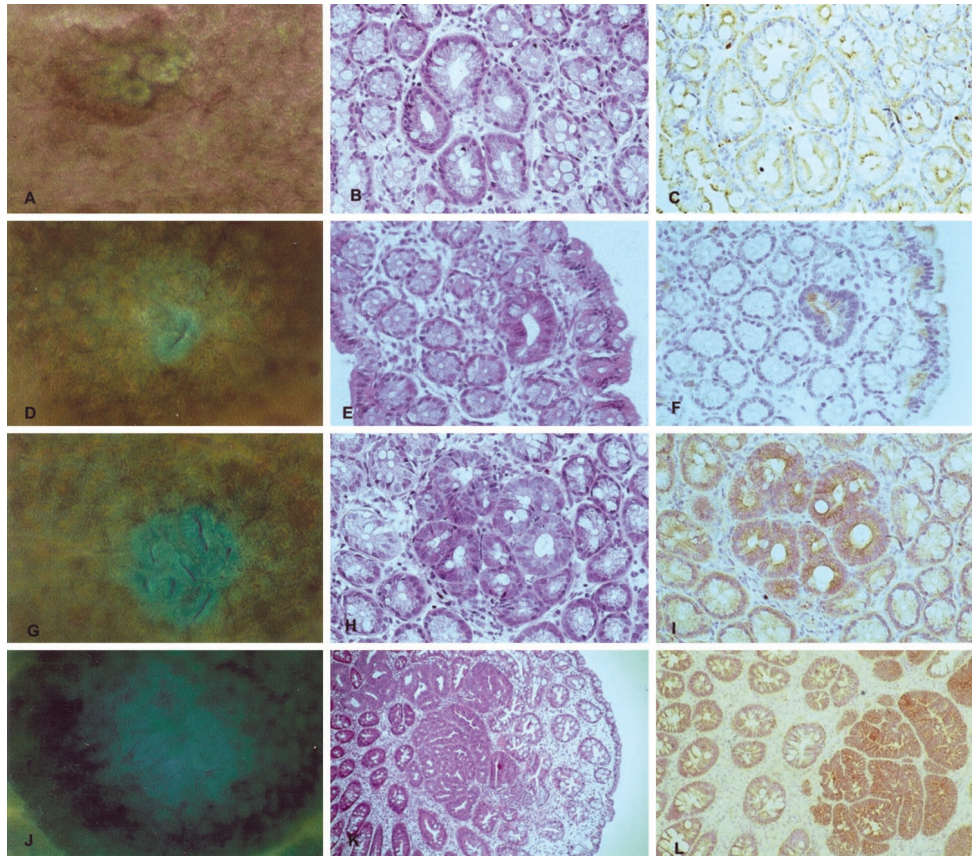

Fig. 1. Morphological features of classical ACF and ACF_{Min} in the colon of AOM-treated mice. Classical ACF were identified in *Min*/+ mice and +/+ mice as *bright blue* and elevated structures by transillumination and surface examination (*A*). In cross-sections (*B*) these lesions were recognized as hyperplastic crypts without β-catenin (*brown color*) overexpression (*C*). Monocryptal ACF_{Min} (*D*) and large ACF_{Min} (*G*) were identified in *Min*/+ mice and +/+ mice as *bright blue* and flat structures by transillumination and surface examination. In cross-sections these lesions were recognized as dysplastic crypts (*E* and *H*) with cytoplasmic overexpression of β-catenin (*F* and *I*) compared with normal adjacent crypts where the β-catenin expression was restricted to the membrane of the cell-cell borders. Tumors (*J*) displayed the same picture of dysplasia (*K*) and altered β-catenin expression (*L*) as ACF_{Min}. The diameter of a histologically normal crypt is ~30 μm.

a large tumor outcome, AOM was given at weeks 1 and 2 after birth, when the *Min*/+ mice are particularly susceptible to carcinogens (21). The morphological relationship between the lesions was examined by histopathology and expression of β-catenin as determined by immunohistochemistry.

MATERIALS AND METHODS

Animals. The mice were bred at the National Institute of Public Health, Oslo, Norway, from inbred mice originally purchased from The Jackson Laboratory (Bar Harbor, ME). The *Min*/+ pedigree was maintained by mating C57BL/6J-+/+ (wild-type) females with C57BL/6J-*Min*/+ males, and procedures to secure inbreeding were followed. The *Min*/+ mice were identified by allele-specific PCR on DNA isolated from blood (21). Water and diet were given *ad libitum*. The mice were given a breeding diet, SDS RM3 (E), from Special Diets Service (Witham, United Kingdom), during gestation and until 5 weeks of age. Thereafter they were given a standard maintenance diet from B&K Universal (Grimston, United Kingdom).

AOM Treatment. AOM from Sigma Chemical Co. (St. Louis, MO) was dissolved in 0.9% NaCl. *Min*/+ mice or their +/+ littermates were given 5 mg/kg body weight AOM s.c. at weeks 1 and 2 after birth, when the animals were particularly susceptible to carcinogens (21). Other groups of mice received similar volumes of the vehicle 0.9% NaCl. The mice were killed by cervical dislocation at 7 or 11 weeks of age.

Scoring of Classical ACF, ACF_{Min}, and Tumors. The colons were removed, rinsed in ice-cold PBS, slit open longitudinally, and fixed flat between wet (PBS) filter papers for 48 h in 10% neutral buffered formalin prior to 30-s staining with 0.2% methylene blue (George T. Gurr Ltd., London, United Kingdom) dissolved in the same formalin solution. At least 24 h after staining, the mucosa was examined by transillumination in an inverse LM (18). Criteria used to identify AC constituting classical ACF were their increased size, bright blue staining, slightly elevated appearance from the surrounding mucosa, and often a more elongated shape of the luminal opening. The size of classical ACF was scored as focal crypt multiplicity (AC/classical ACF). Criteria used to identify aberrant crypts constituting ACF_{Min} were their increased size, bright blue staining, and flat appearance hidden in the surrounding mucosa. Because the ACF_{Min} were not observed as elevated structures, their bright blue staining observed with transillumination was essential for identification. The size of ACF_{Min} was scored as AC/ACF_{Min}. Lesions with more than 12 aberrant crypts were scored as tumors, and their diameters were scored with an eyepiece graticule. The relationship between tumor diameter (d) and crypt multiplicity (c) was empirically determined to be: $c = 0.5 \times d^2$.

Scanning Electron Microscopy. Areas with mucosal lesions, identified by LM surface examination of whole-mount colon preparations, were dissected, washed in PBS, and dehydrated in a graded series of ethanol from 70–100%, before critical point drying (Balzers Union, Balzers, Liechtenstein) from CO_2. The dried specimens were oriented and mounted on stubs under a stereomicroscope and then sputter-coated with platinum. SE was carried out using a JSM 840 SEM [Japan Electron Optical Laboratory (JEOL), Tokyo, Japan] operated at 15 keV.

Histopathological Examination. Areas with mucosal lesions, identified by LM surface examinations of whole-mount colon preparations, were dissected, embedded in paraffin wax, cut in parallel with the mucosal surface, and stained with H&E.

Immunohistochemistry. Paraffin-embedded formalin fixed sections were prepared; deparaffinized; and rehydrated in xylene, graded alcohol, and water. The endogenous peroxidase activity was blocked by incubating the sections in 0.44% hydrogen peroxide for 30 min at room temperature. After the sections were blocked in normal goat serum for 20 min, they were incubated over night at 4°C with mouse monoclonal anti-β-catenin antibody (Transduction Laboratories, Lexington, KY). Then the sections were incubated with goat anti-mouse antibody and ABC-AP reagent according to the manufacturer's instructions (Vectorstain ABC-AP kit; Vector Laboratories, Burlingame, CA). Applying 3,3′-diaminobenzidine tetrahydrochloride containing 0.075% of hydrogen peroxide for 10 min showed peroxidase activity. The sections were stained with hematoxylin for 10 s and mounted with coverslips.

To reduce unspecific coloring we also tried an avidin/biotin blocking kit (Vector Laboratories) to quench the endogenous biotin/avidin and mouse-on-

mouse blocking from Vector M.O.M. immunodetection kit (Vector Laboratories). None of these treatments improved the β-catenin staining or reduced background coloring and were therefore not included in the protocol.

Statistical Analysis. We used a two-way ANOVA (SigmaStat software; Jandel Scientific, Erkrath, Germany), after rank transformation of the data attributable to their non-normal distribution, in order to test the following null hypotheses: (*a*) there is no change from week 7 to 11; and (*b*) there is no effect of gender. The Bonferroni all pairwise multiple comparison procedure was used to isolate the groups that were different. The Mann-Whitney rank order test was used to compare two groups. A $P < 0.05$ was considered significant.

RESULTS

Two Types of ACF. By transillumination and surface examination of whole-mount colon preparations, we identified two types of ACF. In the AOM-treated *Min*/+ mice and +/+ littermates, we detected classical ACF as well as ACF_{Min}. In vehicle-treated *Min*/+ mice controls, we only detected ACF_{Min}, and in vehicle-treated +/+ mice controls, no aberrant crypts of either type were seen. Histopathological and immunohistochemical examination of lesions identified as classical ACF (Fig. 1*A*) revealed normal or hyperplastic crypts (10/10 classical ACF examined; Fig. 1*B*) and no cytoplasmic overexpression of β-catenin (0/10; Fig. 1*C*). The β-catenin expression in these lesions was, as in normal adjacent crypts, restricted to the membrane of the cell-cell borders. In contrast, lesions identified as ACF_{Min} (Fig. 1, *D* and *G*) were uniformly (15/15 ACF_{Min} examined) characterized by moderate to severe dysplasia (Fig. 1, *E* and *H*) and cytoplasmic overexpression of β-catenin (Fig. 1, *F* and *I*) and displayed the same feature in *Min*/+ mice and +/+ mice. The characteristic picture of dysplasia and cytoplasmic β-catenin accumulation in ACF_{Min} was also seen in tumors (Fig. 1, *J–L*) of *Min*/+ mice (6/6 tumors examined) and +/+ mice (2/2 tumors examined). The dysplastic crypts of ACF_{Min} and tumors (Fig. 1, *E*, *H*, and *K*) were characterized by increased crypt diameter, crowding of immature crypt cells, pseudostratification, loss of goblet cells, and a general increase in the size of the nuclei, as we reported previously in untreated *Min*/+ mice (18).

In the lesions with dysplasia and cytoplasmic β-catenin accumulation described above, nuclear translocation of β-catenin was not prominent. To test whether this was attributable to our routine long-term formalin fixation (and storage) of the whole-mount preparations, we treated two *Min*/+ mice with AOM in a second experiment and fixed their preparations ≤24 h in formalin. Surprisingly, the dysplastic lesions in these preparations displayed both cytoplasmic and nuclear accumulation of β-catenin (data not shown), indicating that nuclear immunostaining of β-catenin was dependent on the duration of formalin fixation.

In the SEM, classical ACF were easily observed as elevated lesions (Fig. 2*A*) with similar ultrastructure as the surrounding epithelium, including the presence of goblet cells. In contrast, ACF_{Min} with few crypts displayed enlarged crypts with a flat appearance (Fig. 2*B*). Large ACF_{Min} had enlarged and swollen crypts still with a relative flat appearance (Fig. 2*C*). ACF_{Min} had less goblet cells compared with the background epithelium (Fig. 2*C*).

Formation and Growth of Classical ACF. The number of AOM-induced ACF was significantly higher in Min/+ mice than in +/+ mice at week 7 ($P < 0.01$) but not at week 11 (Table 1). In +/+ mice, the number of ACF was significantly increased from week 7 to 11. The focal crypt multiplicity was significantly increased from week 7 to 11 in both Min/+ mice and +/+ mice ($P < 0.001$, data not shown).

Formation and Growth of ACF_{Min} and Tumors. In *Min*/+ mice treated with AOM, a maximal 13–16-fold increase in ACF_{Min} number at week 7 ($P < 0.002$) and a maximal 18–20-fold increase in tumor number at week 11 ($P < 0.001$) was induced compared with vehicle-treated *Min*/+ controls (Table 1). Apparently there was an association between induction of ACF_{Min} and formation of tumors, because the decrease in ACF_{Min} number from week 7 to 11 corresponded with the increase in tumor number in the same period. Because the number of ACF_{Min} + tumors was virtually constant, it was likely that a large number of ACF_{Min} at week 7 grew to the size of a tumor at week 11. Such a recruitment of newly formed tumors was supported by the smaller mean tumor size found in AOM-treated *Min*/+ mice at week 11 compared with that found in tumors in vehicle-treated *Min*/+ mice ($P < 0.001$; data not shown). To visualize this hypothesis we transformed tumor diameter to crypt multiplicity (see "Materials and Methods"), pooled ACF_{Min} and tumors from both males and females

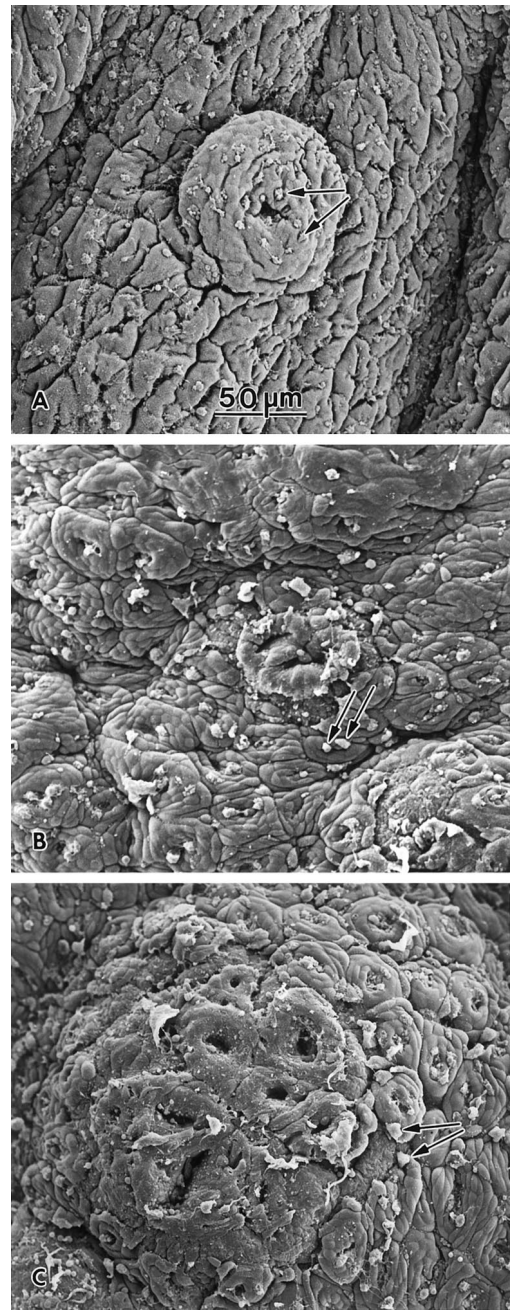

Fig. 2. Scanning electron micrographs of the colonic mucosa of *Min*/+ mice after AOM treatment. *A*, classical ACF recognized as distinct and elevated structures with a similar ultrastructure as the surrounding epithelium. *B*, small ACF_{Min} recognized as enlarged flat crypts. *C*, large ACF_{Min} recognized as enlarged and swollen crypts with a relatively flat appearance and loss of goblet cells compared with the background epithelium. *Arrows*, goblet cells.

Table 1 *Number of lesions in the colon of Min/+ mice and +/+ mice following treatment with AOM or vehicle*

Treatment	Genotype	Lesion	Week 7		Week 11		Two way ANOVA[a]	
			M	F	M	F	Gender	Week
AOM	*Min*/+	Classical ACF	8.3 ± 1.0[b]	7.5 ± 1.0	10.0 ± 2.4	8.3 ± 0.8		
		ACF_{Min}	30.3 ± 5.4	20.8 ± 1.9	7.8 ± 2.4	10.1 ± 1.3		$P < 0.001$
		Tumors	3.4 ± 1.1	0.8 ± 0.3	21.8 ± 4.5	10.5 ± 3.0	$P = 0.002$	$P < 0.001$
			($n = 7$)[c]	($n = 13$)	($n = 6$)	($n = 12$)		
	+/+	Classical ACF	2.9 ± 0.4	4.3 ± 0.6	4.8 ± 1.2	5.8 ± 0.8		$P = 0.018$
		ACF_{Min}	0.7 ± 0.3	0.2 ± 0.2	1.0 ± 0.4	1.3 ± 0.4		$P = 0.038$
		Tumors	0	0	0.3 ± 0.3	0		
			($n = 22$)	($n = 13$)	($n = 6$)	($n = 12$)		
NaCl (control)	*Min*/+	Classical ACF	0	0	0	0		
		ACF_{Min}	2.3 ± 0.4	1.3 ± 0.4	3.1 ± 1.1	2.0 ± 0.6		
		Tumors	0.6 ± 0.2	0.3 ± 0.2	1.1 ± 0.3	0.6 ± 0.2		
			($n = 12$)	($n = 7$)	($n = 7$)	($n = 11$)		
	+/+	Classical ACF	0	0	0	0		
		ACF_{Min}	0	0	0	0		
		Tumors	0	0	0	0		
			($n = 7$)	($n = 10$)	($n = 12$)	($n = 12$)		

[a] Two-way ANOVA test between means in each row to test the following null hypothesis: (*a*) there is no change from week 7 to 11; (*b*) there is no effect of gender. The Mann-Whitney rank order test was used to compare two relevant groups within a column; *P*s are presented in the text.
[b] Mean ± SE.
[c] n = number of animals/group.

in a size distribution plot, and subtracted the size distribution of the *Min*/+ control background (Fig. 3). On the basis of the areas under the curves for the size distributions of AOM-induced lesions at weeks 7 and 11 (Fig. 3*B*), ~56% of the ACF_{Min} at week 7 had grown to the size of a tumor at week 11. With this presumed association between ACF_{Min} growth and tumor formation, the ACF_{Min} (Fig. 3*B*) grew considerably faster than the classical ACF (Fig. 3*A*). This was illustrated by the significantly larger mean crypt multiplicity of pooled ACF_{Min} and tumors at week 11 compared with the corresponding mean crypt multiplicity of classical ACF (33.4 ± 2.6, $n = 418$ *versus* 6.2 ± 0.3, $n = 157$, $P < 0.001$).

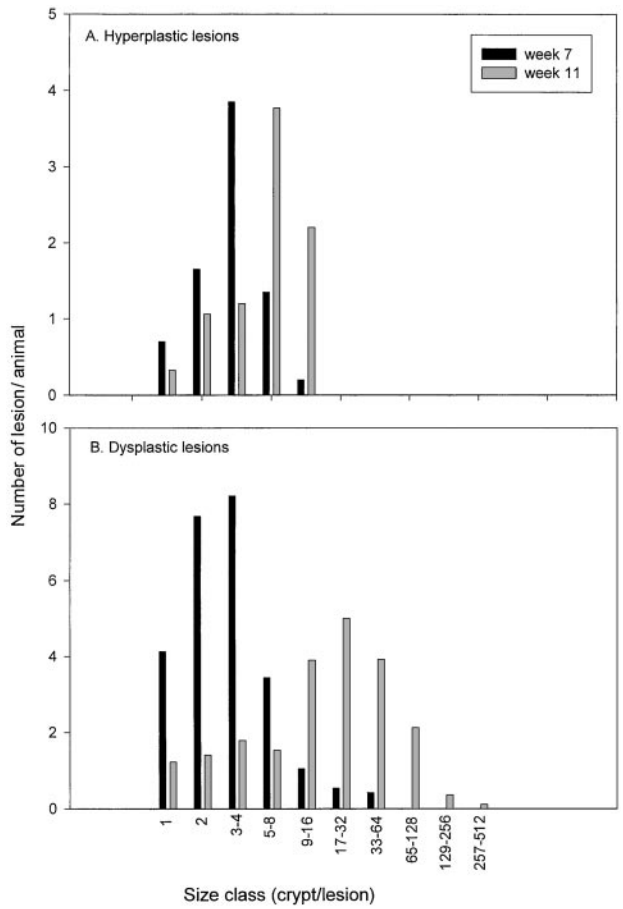

Fig. 3. Size distribution of hyperplastic lesions and dysplastic lesions at weeks 7 and 11 from pooled male and female *Min*/+ mice after AOM treatment. *A*, the hyperplastic lesions are equivalent with classical ACF. *B*, dysplastic lesions are equivalent with ACF_{Min} + tumors. The size is expressed as crypt multiplicity (*crypt/lesion*), and each size class unit represents a successively doubling of crypts. The size distribution of spontaneous lesions in NaCl-treated *Min*/+ mice (controls) is subtracted from the size distribution of AOM-treated *Min*/+ mice. Tumor diameter (d) was transformed to crypt multiplicity (c) by the formula: $c = 0.5 \times d^2$.

Also in +/+ mice, the AOM treatment resulted in the induction of ACF_{Min} and tumors. However, the number of these lesions was at the same low level as in control *Min*/+ mice.

DISCUSSION

By transillumination and surface examination of whole-mount colon preparations of AOM-treated *Min*/+ mice, we were able for the first time to identify specific lesions that show a continuous development from the monocryptal stage to adenoma. We called these lesions ACF_{Min} because we first discovered them in untreated *Min*/+ mice (18). The uniform picture of dysplasia and cytoplasmic overexpression of β-catenin in monocryptal ACF_{Min}, large ACF_{Min}, and adenomas indicated a qualitative relationship between ACF_{Min} and tumorigenesis. A quantitative relationship was also observed because the dramatic decrease in ACF_{Min} number from week 7 to 11 was paralleled by a reciprocal increase in tumor number. By calculating the crypt multiplicity of ACF_{Min} and tumors pooled, we determined a high growth rate for ACF_{Min}. In all of the AOM-treated *Min*/+ mice, it was possible to distinguish ACF_{Min} from classical ACF, which were not dysplastic and did not display cytoplasmic accumulation of β-catenin. The number of classical ACF was virtually constant between week 7 and 11, the focal crypt multiplication of classical ACF was modest and they were not found in untreated *Min*/+ mice. Therefore, in contrast to ACF_{Min}, the classical ACF did not seem to be related to tumorigenesis.

Contrary to what was reported for tumors of *Min*/+ mice (17), we did not see significant nuclear immunostaining of β-catenin in the dysplastic lesions. This was probably related to the long-term formalin fixation applied in the present study, because nuclear immunostaining of β-catenin was indeed confirmed in dysplastic lesions from an additional experiment where the preparations were fixed no longer than 24 h. This is in concurrence with a previous study demonstrating that the immunohistochemical detection of nuclear β-catenin in colorectal tumors may be dependent on the method of fixation (22).

The fact that AOM treatment led to the formation of ACF_{Min} in

both *Min*/+ mice and in +/+ mice indicated that these lesions are general precursors of adenomas in the colon. Although the ACF_{Min} and tumors in both *Min*/+ mice and in +/+ mice were characterized by altered β-catenin accumulation, the initiating mechanisms induced by AOM might be different in the two genotypes. In *Min*/+ mice, which harbor only one intact *Apc* allele, it is likely that the formation of ACF_{Min} is initiated by the inactivation of the remaining wild-type *Apc* allele, leaving the crypt cell with lost Apc function. Such a mechanism, which implies that the *Min*/+ mice are more vulnerable than +/+ mice to AOM treatment, is consistent with the 50–100-fold higher frequency of ACF_{Min} observed in *Min*/+ mice than in +/+ mice at week 7. Accordingly, the tumor frequency at week 11 was ~100-fold higher in *Min*/+ mice than in +/+ mice. Furthermore, genetic analyses of lesions from untreated *Min*/+ mice (5–7) and *Min*/+ mice treated with *N*-ethyl-*N*-nitrosourea (23) suggest that intestinal tumorigenesis in these animals are dependent on somatic events that lead to the inactivation of both *Apc* alleles. On the other hand, in AOM-treated +/+ mice, which harbor two intact *Apc* alleles, it is more likely that *β-catenin* gene mutation rather than "two hits" at the *Apc* locus is the main cause of lost β-catenin control. This speculation accords with results from other studies in wild-type rodents. Interestingly, the morphological feature of ACF_{Min} appears identical to the histologically altered crypts with macroscopically normal-like appearance recently identified in early rat colon carcinogenesis induced by AOM (14). Histologically altered crypts with macroscopically normal-like appearance, which could not be distinguished from normal adjacent crypts in whole-mount preparations examined by surface microscopy, were characterized by altered β-catenin control and frequent *β-catenin* gene mutations. Such alterations in β-catenin were also observed in colonic tumors from rat and mouse (15–17). Additional genetic analyses of ACF_{Min} in *Min*/+ mice and +/+ mice are required to elucidate the mechanisms for their altered β-catenin accumulation.

We described previously ACF_{Min} in the colon of untreated *Min*/+ mice as flat structures that could not be recognized in the SEM (21). In the present study, we could identify large ACF_{Min} by scanning electron microscopy probably because the lesions had developed large, swollen crypts that were slightly elevated upon expansion in the mucosa. Disrupted Apc control of the β-catenin/Tcf pathway, a signal that is essential for the maintenance of the proliferative compartments of the intestine during embryogenesis (24), may explain the immature (dysplastic) appearance of crypt cells constituting ACF_{Min}. The relative flat appearance of ACF_{Min} could be a result of disrupted Apc control of the cell cycle (25) and cell anchoring (26), as well as disrupted Apc-driven migration (27) and apoptosis (28). Furthermore, ACF_{Min} resemble a subset of ACF, the dysplastic ACF, that are described previously as potential precursors of adenomas in rodent and human colon carcinogenesis (7, 10, 13, 29). Interestingly, these dysplastic ACF, which are characterized by their larger size (13, 29), accord with the fast growing ACF_{Min} in our study. If these dysplastic ACF initially possess a flat morphology like small ACF_{Min}, they might not be identified by conventional ACF scoring. However, at later stages they might be scored, as slightly elevated structures with dysplasia, like large ACF_{Min}.

The induction of classical ACF by AOM was apparently not affected by *Apc* status because the number of these lesions was approximately the same in *Min*/+ and +/+ mice, and because they displayed normal β-catenin expression. The classical ACF in our experiment resemble the previously described hyperplastic ACF, which are not assumed to be precursors of adenomas (9). These hyperplastic lesions, which constitute the majority of ACF, are characterized by mutations in *ras* (7, 9, 30) rather than in *Apc* (7) or *β-catenin* (14). These lesions are frequent in tumor resistant mice treated with AOM (31) and in non-neoplastic colonic disease (27).

In conclusion, we identified two distinct populations of altered crypts, ACF_{Min} and classical ACF, in the colon of *Min*/+ mice after AOM treatment. Apparently, these populations represent separate directions of development already from the monocryptal stage. The ACF_{Min}, which resemble the dysplastic ACF described previously, demonstrated a continuous development from the monocryptal stage to adenoma with fast crypt multiplication and altered control of β-catenin. At the initial stage, the dysplastic lesions were flat structures hidden in the surrounding mucosa and therefore not detectable as ACF by conventional methods. In contrast, the classical ACF, which resemble the hyperplastic ACF as described in the literature, were characterized by slow growing crypts with normal β-catenin expression, and they were probably not related to tumorigenesis. Additional studies are warranted to characterize the phenotypic and genotypic features of both types of ACF and their relationship to colonic carcinogenesis in FAP as well as in sporadic colorectal cancer.

ACKNOWLEDGMENTS

We thank Marit Hindrum and Ingeborg Løstegaard Goverud for excellent technical assistance.

REFERENCES

1. Kinzler, K. W., and Vogelstein, B. Lessons from hereditary colorectal cancer. Cell, *87:* 159–170, 1996.
2. Miyoshi, Y., Nagase, H., Ando, H., Horii, A., Ichii, S., Nakatsuru, S., Aoki, T., Miki, Y., Mori, T., and Nakamura, Y. Somatic mutations of the APC gene in colorectal tumors: mutation cluster region in the APC gene. Hum. Mol. Genet., *1:* 229–233, 1992.
3. Paulsen, J. E. Modulation by dietary factors in murine FAP models. Toxicol. Lett. (Amst.), *112–113:* 403–409, 2000.
4. Su, L-K., Kinzler, K. W., Vogelstein, B., Preisinger, A. C., Moser, A. R., Luongo, C., Gould, K. A., and Dove, W. F. Multiple intestinal neoplasia caused by a mutation in the murine homolog of the APC gene. Science (Wash. DC), *256:* 668–670, 1992.
5. Luongo, C., Moser, A. R., Gledhill, S., and Dove, W. F. Loss of Apc^{+} in intestinal adenomas from Min mice. Cancer Res., *54:* 5947–5952, 1994.
6. Levy, D. B., Smith, K. J., Beaser-Barclay, Y., Hamilton, S. R., Vogelstein, B., and Kinzler, K. W. Inactivation of both *APC* alleles in human and mouse tumors. Cancer Res., *54:* 5953–5958, 1994.
7. Jen, J., Powell, S. M., Papadopoulos, N., Smith, K. J., Hamilton, S. R., Vogelstein, B., and Kinzler, K. W. Molecular determinants of dysplasia in colorectal lesions. Cancer Res., *54:* 5523–5526, 1994.
8. Wargovich, M. J., Jimenez, A., McKee, K., Steele, V. E., Velasco, M., Woods, J., Price, R., Gray, K., and Kelloff, G. J. Efficacy of potential chemopreventive agents on rat colon aberrant crypt formation and progression. Carcinogenesis (Lond.), *21:* 1149–1155, 2000.
9. Nucci, M. R., Robinson, C. R., Longo, P., Campell, P., and Hamilton, S. R. Phenotypic and genotypic characteristics of aberrant crypt foci in human colorectal mucosa. Hum. Pathol., *28:* 1396–1407, 1997.
10. Siu, I-M., Pretlow, T. G., Amini, S. B., and Pretlow, T. P. Identification of dysplasia in human colonic aberrant crypt foci. Am. J. Pathol., *150:* 1805–1813, 1997.
11. Kristinsson, J., Røseth, A. G., Sundset, A., Nygaard, K., Løberg, E. M., Paulsen, J. E., Aadland, E., and Fagerhol, M. K. Granulocyte marker protein is increased in stools from rats with azoxymethane-induced colon cancer. Scand. J. Gastroenterol., *34:* 1216–1223, 1999.
12. Cameron, I. L., Garza, J., and Hardman, W. E. Distribution of lymphoid nodules, aberrant crypt foci and tumours in the colon of carcinogen-treated rats. Br. J. Cancer, *73:* 893–898, 1996.
13. Thorup, I. Histomorphological and immunochemical characterization of colonic aberrant crypt foci in rats: relation to growth factor expression. Carcinogenesis (Lond.), *18:* 465–472, 1997.
14. Yamada, Y., Yoshimi, N., Hirose, Y., Kawabata, K., Matsunaga, K., Shimizu, M., Hara, A., and Mori H. Frequent *β-catenin* gene mutations and accumulations of the protein in the putative preneoplastic lesions lacking macroscopic aberrant crypt foci appearance in rat colon carcinogenesis. Cancer Res., *60:* 3323–3327, 2000.
15. Takahashi, M., Fukuda, K., Sugimura, T., and Wakabayashi, K. β-Catenin is frequently mutated and demonstrates altered cellular location in azoxymethane-induced rat colon tumors. Cancer Res., *58:* 42–46, 1998.
16. Takahashi, M., Nakatsugi, S., Sugimura, T., and Wakabayashi, K. Frequent mutations of the *β-catenin* gene in mouse colon tumors induced by azoxymethane. Carcinogenesis (Lond.), *21:* 1117–1120, 2000.
17. Sheng, H., Shao, J., Williams, C. S., Pereira, M. A., Taketo, M. M., Oshima, M., Reynolds, A. B., Washington, M. K., DuBois, R. N., and Beauchamp, R. D. Nuclear translocation of β-catenin in hereditary and carcinogen-induced intestinal adenomas. Carcinogenesis (Lond.), *19:* 543–549, 1998.

18. Paulsen, J. E., Namork, E., Steffensen, I-L., Eide, T. J., and Alexander, J. Identification and quantification of aberrant crypt foci in the colon of Min mice–a murine model of familial adenomatous polyposis. Scand. J. Gastroenterol., *35:* 534–539, 2000.
19. Paulsen, J. E., Namork, E., Steffensen, I-L., and Alexander, J. Morphological discrepancy between spontaneous and azoxymethane-induced aberrant crypts in the colon of MIN mice. Proc. Am. Assoc. Cancer Res., *37:* 110, 1996.
20. Humpage, A. R., Hardy, S. J., Moore, E. J., Froscio, S. M., and Falconer, I. R. Microcystins (cyanobacterial toxins) in drinking water enhance the growth of aberrant crypt foci in the mouse colon. J. Toxicol. Environ. Health Part A, *61:* 155–165, 2000.
21. Paulsen, J. E., Steffensen, I-L., Andreassen, Å., Vikse, R., and Alexander, J. Neonatal exposure to the food mutagen 2-amino-1-methyl-6-phenylimidazo [4,5-*b*] pyridine via breast milk or directly induces intestinal tumors in multiple intestinal neoplasia mice. Carcinogenesis (Lond.), *20:* 1277–1282, 1999.
22. Munné, A., Fabre, M., Marinoso, M. L., Gallén, M., and Real, F. X. Nuclear β-catenin in colorectal tumors: to freeze or not to freeze? J. Histochem. Cytochem., *47:* 1089–1094, 1999.
23. Shoemaker, A. R., Luongo, C., Moser, A. R., Marton, L. J., and Dove, W. F. Somatic mutational mechanisms involved in intestinal tumor formation in Min mice. Cancer Res., *57:* 1999–2006, 1997.
24. Korinek, V., Barker, N., Moerer, P., van Donselaar, E., Huls, G., Peters, P. J., and Clevers, H. Depletion of epithelial stem-cell compartments in the small intestine of mice lacking Tcf-4. Nat. Genet., *19:* 379–381, 1998.
25. Baeg, G-H., Matsumine, A., Kuroda, T., Bhattachajee, R. N., Miyashiro, I., Toyoshima, K., and Akiyama, T. The tumour suppressor gene product APC blocks cell cycle progression from G_0/G_1 to S phase. EMBO J., *14:* 5618–5625, 1995.
26. Wong, M. H., Hermiston, M. L., Syder, A. J., and Gordon, J. I. Forced expression of the tumor suppressor adenomatosis coli protein induces disordered cell migration in the intestinal epithelium. Proc. Natl. Acad. Sci. USA, *93:* 9588–9593, 1996.
27. Näthke, I. S., Adams, C. L., Polakis, P., Sellin, J. H., and Nelson, W. J. The adenomatous polyposis coli tumor suppressor protein localizes to plasma membrane sites involved in active cell migration. J. Cell Biol., *134:* 165–179, 1996.
28. Morin, P. J., Vogelstein, B., and Kinzler, K. W. Apoptosis and APC in colorectal tumorigenesis. Proc. Natl. Acad. Sci. USA, *93:* 7950–7954, 1996.
29. Bouzourene, H., Chaubert, P., Seelentag, W., Bosman, F. T., and Saraga, E. Aberrant crypt foci in patients with neoplastic and non-neoplastic colonic diseases. Hum. Pathol., *30:* 66–71, 1999.
30. Bolt, A. B., Papanikolaou, A., Delker, D. A., Wang, Q-S., and Rosenberg, D. W. Azoxymethane induces KI-ras activation in tumor resistant AKR/J mouse colon. Mol. Carcinog., *27:* 210–218, 2000.
31. Papanikolaou, A., Wang, Q-S., Papanikolaou, D., Whiteley, H. E., and Rosenberg, D. W. Sequential and morphological analyses of aberrant crypt foci formation in mice of differing susceptibility to azoxymethane-induced colon carcinogenesis. Carcinogenesis (Lond.), *21:* 1567–1572, 2000.

Qualitative and Quantitative Relationship between Dysplastic Aberrant Crypt Foci and Tumorigenesis in the *Min*/+ Mouse Colon

Jan Erik Paulsen, Inger-Lise Steffensen, Else Marit Løberg, et al.

Cancer Res 2001;61:5010-5015.